Fire Ecology

ORIGINAL RESEARCH

Open Access

Forest fire pattern and vulnerability mapping using deep learning in Nepal

Bhogendra Mishra[1,2]* , Saroj Panthi[3], Shobha Poudel[1,2] and Bhoj Raj Ghimire[2,4,5]

Abstract

Background In the last two decades, Nepal has experienced an increase in both forest fire frequency and area, but very little is known about its spatiotemporal dimension. A limited number of studies have researched the extent, timing, causative parameters, and vulnerability factors regarding forest fire in Nepal. Our study analyzed forest fire trends and patterns in Nepal for the last two decades and analyzed forest fire-vulnerability risk based on historical incidents across the country.

Results We analyzed the spatial and temporal patterns of forest fires and the extent of burned area using the Mann-Kendall trend test and two machine-learning approaches maximum entropy (MaxEnt), and deep neural network (DNN). More than 78% of the forest fire burned area was recorded between March and May. The total burned area has increased over the years since 2001 by 0.6% annually. The forest fire-vulnerability risk obtained from both approaches was categorized into four classes—very high, high, low, and very low.

Conclusions Although burned area obtained from both models was comparable, the DNN slightly outperformed the MaxEnt model. DNN uses a complex structure of algorithms modeled on the human brain that enables the processing of the complex relationship between input and output dataset, making DNN-based models recommended over MaxEnt. These findings can be very useful for initiating and implementing the most suitable forest management intervention.

Keywords Climatic condition, Forest fire, MaxEnt, MODIS, Nepal

*Correspondence:
Bhogendra Mishra
bhogendra@gmail.com
[1] Policy Research Institute, Narayanhiti, Kathmandu, Nepal
[2] Science Hub, Kathmandu, Balaju, Nepal
[3] Ministry of Forest, Environment and Soil Conservation, Pokhara, Gandaki Province 33700, Nepal
[4] Nepal Open University, Kathmandu, Kumaripati-Mahalaximisthan Road, Lalitpur 44700, Nepal
[5] Regional Integrated Multi-Hazard Early Warning System for Africa and Asia, Klong Nueng, Klong Luang, Thailand

Mishra *et al. Fire Ecology*   (2023) 19:3

Page 2 of 15

Resumen

Antecedentes En las últimas dos décadas, Nepal ha experimentado un incremento tanto en la frecuencia como en área afectada por incendios forestales, aunque se conoce muy poco sobre su dimensión espacio-temporal. Un número limitado de estudios ha investigado sobre la extensión, el tiempo de ocurrencia, los parámetros causales, y los factores de vulnerabilidad en relación a los incendios forestales en Nepal. Nuestro trabajo analizó las tendencias en los incendios forestales y los patrones en Nepal de las últimas dos décadas y analizó la vulnerabilidad al riesgo de incendios forestales basados en incidentes históricos a través de todo el país.

Resultados Analizamos el patrón espacial y temporal de los incendios, y la extensión del área afectada usando la tendencia de Mann-Kendall y dos aproximaciones de aprendizaje automático (machine learning) de máxima entropía (MaxEnt), y la red neuronal profunda (DNN). Más de 78% del área de bosques quemada fue registrada entre marzo y mayo. El área total quemada se incrementó desde 2001 a una tasa del 0,6% anual. El riesgo de vulnerabilidad de incendios forestales obtenido mediante las dos aproximaciones fue categorizado en cuatro clases – muy alta, alta, baja, y muy baja.

Conclusiones Aunque el área quemada obtenida mediante los dos modelos es comparable, el DNN superó ligeramente al modelo MaxEnt. El DNN usa una compleja estructura de algoritmos modelados en el cerebro humano que permite el procesamiento las complejas relaciones entre los ingresos y egresos del conjunto de datos, haciendo a los modelos basados en DNN más recomendables sobre el MaxEnt. Estos hallazgos pueden ser útiles para iniciar e implementar las intervenciones forestales más adecuadas.

Introduction

Forest fire not only significantly contributes to anthropogenic greenhouse gas emissions, but also adversely affects wildlife, ecosystem, and watershed management. It is a disaster with major environmental and ecological impacts that threaten human lives and livelihoods. About 7.2 billion ha of land (i.e., forests, other wooded lands, and other lands) was burned in 2001–2018 globally at an average of about 400 million ha per year (Robinne 2021). The annual burned area from 2013 to 2018 was less than the long-term average (FAO 2020). Another study showed that the global burned area has declined by 24.3 ± 8.8% over the past 18 years (Andela et al. 2017), but a re-analysis of the ensembles with climate models showed that forest fire risk increased by about 1.1 times in current climate conditions in comparison to pre-industrial climate conditions, and for future climate conditions (2 °C global temperature increment), it could increase by two times (Aponte et al. 2016). Every year, many people are killed due to forest fire, and this number has been increasing over the years (Doerr and Santín 2016).

Apart from the impact of fire on emissions, forest fire is a major driver of deforestation and land degradation. Increased runoff, floods, and landslides are consequences of forest fire (American Forest Foundation 2015). It also causes significant economic loss. As estimated by the Economy and Environment Program for Southeast Asia, the cost of damages from Southeast Asian fires is more than $4.5 billion (Cotton 2014).

According to the historical dataset in Nepal, about 40,000 ha of forest area is burned in Nepal every year. The majority of forest fire incidents and affected areas are recorded between March and May (Matin et al. 2017). The dry season (February through May) is very susceptible to forest fire due to low rainfall and high temperature; consequently, tackling a forest fire in this season is challenging in Nepal. The year 2009 had the worst record of forest fire, causing 41 casualties and severe damage in human settlements and forests in Nepal (GON 2014).

Anthropogenic activities are identified as major sources of ignition of forest fires (Bahadur et al. 2017); however, prolonged dry winters and increasing frequency of droughts in the spring are major causes of forest fire spread in Nepal. The forest fires could be deliberate, due to negligence or accidental (Kunwar and Khaling 2006). Many land managers deliberately ignite forests to promote new shoots of grass, to clear vegetation for better sight of prey, or to expand agricultural lands. Unintentional or accidental forest fire often occurs from careless handling of burning match sticks or cigarette buts, children set fires unknowingly, leaving extinguished fire by charcoal makers, and fire remained after campfire or picnic (Gentle 1997; Kunwar and Khaling 2006).

With the advancement of technology, the availability of remotely sensed data on forest cover and bioclimatic and anthropogenic variables has increased since the beginning of this century. Remotely sensed data have been very helpful for quantitative studies on the impact of bioclimatic

variables in forest fires. These data have been widely used for the study of different aspects of forest fires such as active fire monitoring, risk monitoring, and understanding causes and effects, among others (Bowman and Murphy 2010; Nelson and Chomitz 2011; Matin et al. 2017).

Forest fire modeling tools are crucial to the identification and visualization of forest fire distribution based on scientific methods. Some popular tools include Multidimensional Scaling (MDS) visualization tool, hexagonal cellular automata, maximum entropy (MaxEnt), random forest, a regression tree analysis, and deep learning methods (Hernández Encinas et al. 2007; Lopes and Machado 2014; Miquelajauregui et al. 2016; Leuenberger et al. 2018; Kim et al. 2019; Zhang et al. 2019). The MaxEnt model needs only presence points for modeling purposes (Phillips et al. 2006); therefore, this has been the most frequently used model (Biswas et al. 2015; Fonseca et al. 2017). The MaxEnt model uses a general-purpose machine-learning method with a simple and precise mathematical formulation (Phillips et al. 2006). Although the MaxEnt model was introduced as a species distribution tool, it is successfully used to model forest fire-vulnerability risk in a diverse environment (Renard et al. 2012; De Angelis et al. 2015; Fonseca et al. 2017; Kim et al. 2019; Martín et al. 2019; Makhaya et al. 2022). In a comparative study on forests in South Korea and Spain, MaxEnt outperformed random forest and generalized linear models (GLM) (Vilar et al. 2016; Kim et al. 2019).

On the other hand, deep-learning-based approaches such as deep neural network (DNN) and convolution neural networks (CNN), among others, are outperforming many other machine-learning methods for diverse applications in recent years (Mishra et al. 2022; Zhang et al. 2021). However, their applicability has not been fully explored in the case of forest fire modeling. Moreover, DNN could be more effective in extracting the information (pattern) from the large datasets of bioclimatic, topographic, and anthropogenic variables required to cover an entire country (Jain et al. 2020).

Very limited studies have been done on forest fires in Nepal, and many of them focused on a small geographical extent (Khanal 2015; Matin et al. 2017; Parajuli et al. 2020). The relationship between forest fire and potential causative parameters is not well explored in the complex mountainous topography of Nepal. Identifying the relationship of bioclimate, anthropogenic causes, topography, and vegetation indices to forest fire is important to map forest fire-vulnerability risk. It helps to define relative risk at specific locations that can aid in developing better forest fire management plans to minimize threats to life, property, and natural resources (Poudel et al. 2020). To fill the gap, this study leveraged remote-sensing data and technologies to analyze forest fire regime over time (monthly) and space

(physiographic regions of Nepal) between the years 2001 and 2019 and developed a fire-vulnerability map based on the historical forest fire dataset.

The main objective of this study was to model the forest fire-vulnerability risk of Nepal using historical forest fire incidents based on MODIS data. To obtain this objective, the following sub-objectives were to (1) analyze the forest fire trend in different physiographic regions of Nepal and (2) model forest fire-vulnerability risk across Nepal with DNN using historical data and comparing the results with those from the widely accepted MaxEnt modeling tool.

Materials and methods
Study area
The study was conducted throughout Nepal's forested area. Nepal is situated in the central part of the Himalayas, between 26° 22′ and 30° 27′ N latitudes and 80° 04′ and 88° 12′ E longitudes, covering an area of 147,516 km² with elevation varying between 70 and 8848 m. It is divided into five physiographic zones: High Mountains, Middle Mountains, Hills, Chure (known locally as Siwalik), and Terai. Politically, it is divided into seven provinces and 753 local administrative units that include municipalities, rural-municipalities, sub-metropolitan, and metropolitan cities.

Nepal has tremendous geographic diversity that ranges from tropical alluvial plains in the south to the very rugged and permanently snow- and ice-covered Himalayan Mountains in the north. The climate varies from alpine cold, semi-desert type in the trans-Himalayan zone to a humid tropical type in the tropical lowlands in the south (GON 2014). It has been observed that the temperature varies greatly from south to north, as it does along elevation zones. The High Mountains are the coldest region, with below 0 °C throughout the year, whereas the Terai region has the highest temperatures that can reach up to 46 °C. Eighty percent of the precipitation that falls in Nepal comes in the form of summer monsoon rain, from June to September (Bhuju et al. 2007; Mishra et al. 2014; Poudel et al. 2017).

The country receives an average annual rainfall of around 1600 mm (Bhuju et al. 2007; GON 2014; Mishra et al. 2014). The mean annual precipitation of the country varies spatially; specifically, less precipitation falls in the northern regions than in the southern plain. Similarly, during monsoon season, precipitation in the western part is less than that in the eastern part.

For this study, the High Mountains zone was not considered because the occurrence of forest is very rare at very high elevations. Hence, the study and analysis were conducted in four physiographic regions: Middle Mountains, Hills, Chure, and Terai.
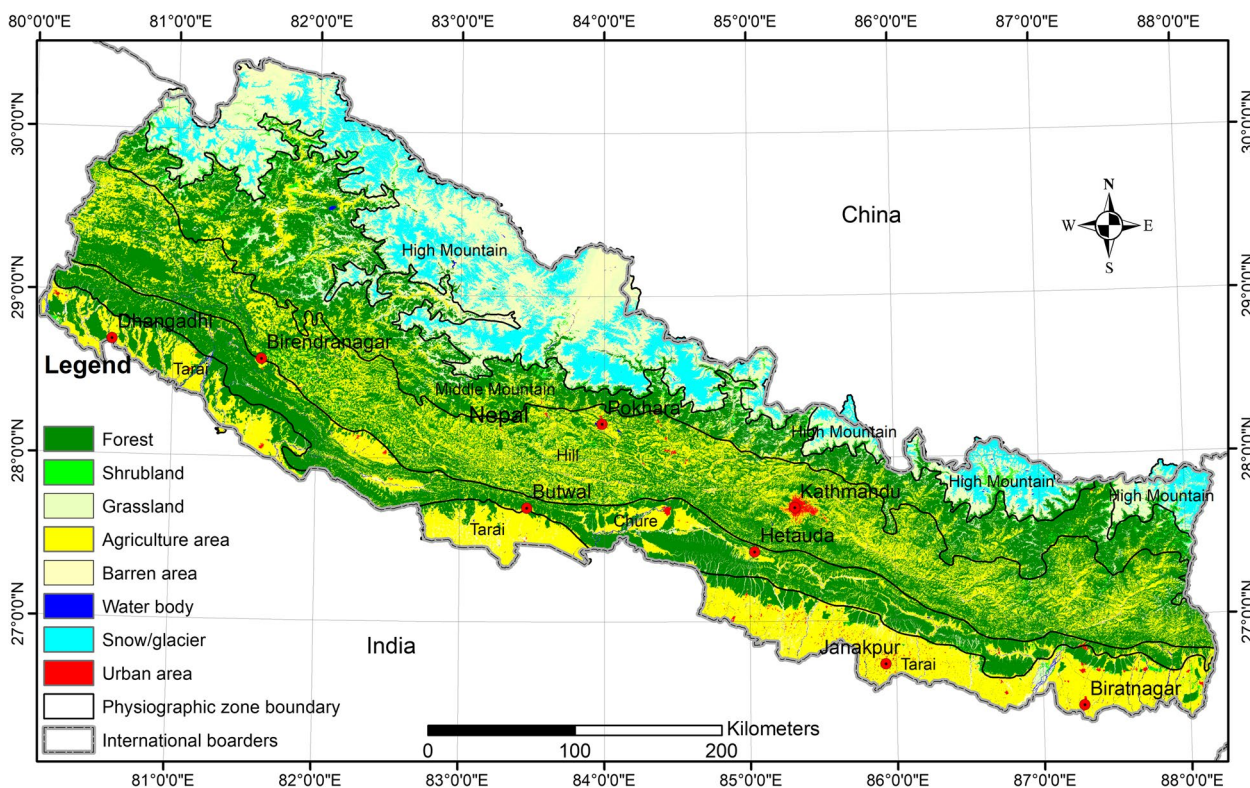
Mishra *et al. Fire Ecology* (2023) 19:3

Page 4 of 15

Fig. 1 Land cover map (2000) of Nepal that we used to model forest fire-vulnerability risk of the country using historical forest fire data

- The Terai is the lower part of Nepal, which extends south of Chure to the northern part of the Indo-Gangetic plain. Its average elevation is less than 750 m. It has a tropical climate and is mostly very densely populated or covered by tropical forest.
- The Chure, sandwiched between Terai and Hills, extends east to west at about the 700- to 1500-m elevation. It has a subtropical climate and is covered by a large forest.
- Hills, locally known as the Mahabharat Range, runs through the center of the country with green mountains, river duns, and valleys. Sandwiched between Chure and the Middle Mountains zone, Hills has a warm temperate climate, and the elevation varies between 1500 and 2700 m.
- The Middle Mountains zone consists of the seasonally snow-covered mountainous area with sparse forests and bushes, ranges from 2200 to 4000 m, and has a subalpine climate.

The area above 4000 m and up to 8848 m is the Himalaya, with an alpine climate and no or only seasonal vegetation. All physiographic zones run continuously from east to west, with a few breaks only in Terai, as shown in Fig. 1.

Broad-leaved forests are dominated by *Shorea robusta* Roth (sal) and *Terminalia elliptica* Willd. (saaj) in the Terai. Chure's broad-leaved forest is dominated by *Shorea robusta* and *Pinus roxburghii* Sarg.(chir pine). Subtropical and temperate, subalpine and alpine, and Nival vegetation are found in Hills, Middle Mountains, and High Mountains zones, respectively (Dobremez 1976). The government of Nepal has also developed the forest inventory according to the five designated physiographic zones. Twenty protected areas of Nepal cover 23.39% of the total land of the country, and that is mostly forest and extends into all physiographic zones (FRA/DFRS 2015).

Data used
Forest fire data
MODIS monthly fire product (MCD45A1), a global product of 500-m spatial resolution that includes quality index (Boschetti et al. 2008), was used in this study. This is the product of the daily TERRA and AQUA satellites used all over the world. It has already been used and validated in the study of forest fire in several places in the world, including Nepal (De Araújo and Ferreira 2015; Fornacca et al. 2017; Matin et al. 2017). Only the burned areas with the highest confidence rating (quality index flag 1) were considered in this study (Fig. 2a). In addition
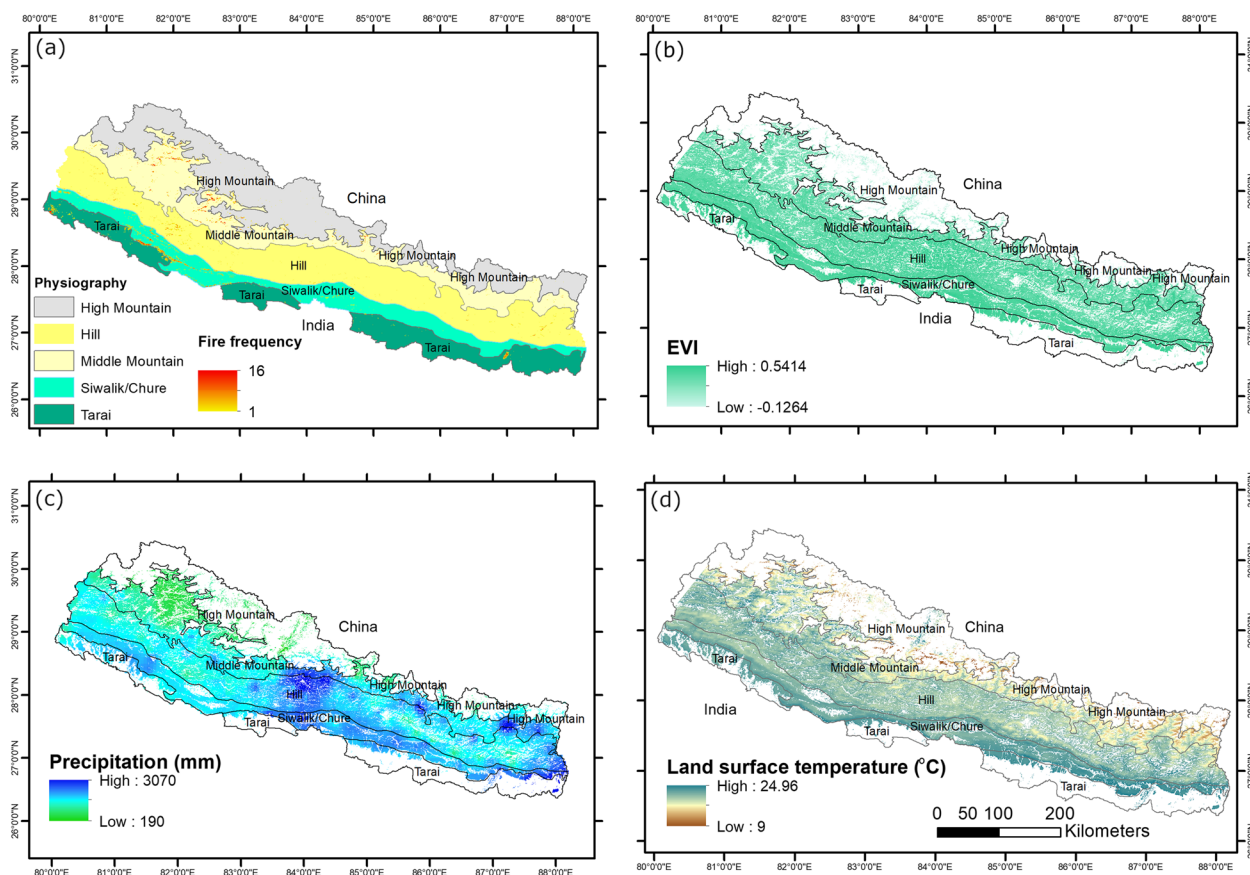
Mishra *et al. Fire Ecology*   (2023) 19:3

Page 5 of 15

Fig. 2 Maps illustrating **a** fire incident frequency and area burned, **b** enhanced vegetation index (EVI), **c** average annual precipitation (mm), and **d** average annual land surface temperature (°C) of Nepal

to that, the event of fire occurrence data were obtained from the Forest Fire Detection and Monitoring System of Nepal, developed and maintained by the Ministry of Forest and Environment, Department of Forest and Soil Conservation from 2017 to 2019 (DoF 2022).

Forest cover area and vegetation dataset

International Centre for Integrated Mountain Development (ICIMOD) land use and cover map (ICIMOD 2018) was used as the baseline map for forest and vegetation cover in 2000; all forest fire incidents were examined with regard to this mapped forested area. The time series global MODIS 250-m vegetation products (MOD13Q1/MYD13Q1) were used for computing the mean annual Normalized Difference Vegetation Index (NDVI) value. This product has been used in a large number of applications for forest and agricultural land monitoring in several parts of the world, including Nepal (Boschetti et al. 2008; Ghimire et al. 2017; Luintel et al. 2021). Based on the forest phenology, the low NDVI value indicates that water-stressed vegetation is more fire prone than vegetation that has a higher NDVI (Kasischke et al. 1993; Illera et al. 1996).

Bioclimatic variables

We considered 19 bioclimatic variables that were identified as the contributing factors for forest fire in this study. These variables have been identified as the governing factors for the spread of forest fire in several parts of the world (Furlaud et al. 2021; Singh and Zhu 2021; Makhaya et al. 2022). These bioclimatic datasets were acquired from WorldClim's Global Climate Data website (http://worldclim.org/version2), which are well-accepted datasets used for forest fire application (Fick and Hijmans 2017). The bioclimatic data are 30 arc seconds (~1 km) spatial resolution. The details of these datasets are presented in Table 1.

Topographical variables

Similar to bioclimatic variables, a number of topographic variables are identified as contributing factors for forest fire in several parts of the world (Makhaya et al. 2022). A digital elevation model (DEM) of 30-m resolution was downloaded from EarthExplorer (https://earthexplorer.usgs.gov/). Aspect and slope were calculated from the DEM using Arc-GIS software (ESRI 2017; ESRI, Redlands, California, USA).

Mishra *et al. Fire Ecology*   (2023) 19:3

Page 6 of 15

Table 1 Environmental variables used for modeling forest fire-vulnerability risk of Nepal. Abbreviations used in text and variable units are also given

Category	Data source	Variables	Abbreviation	Units
Bioclimatic	**WorldClim**	Annual mean temperature	Bio1	°C
		Mean diurnal range	Bio2	°C
		Isothermality	Bio3	Dimensionless
		Temperature seasonality (standard deviation)	Bio4	°C
		Maximum temperature of warmest month	Bio5	°C
		Minimum temperature of coldest month	Bio6	°C
		Annual temperature range	Bio7	°C
		Mean temperature of wettest quarter	Bio8	°C
		Mean temperature of driest quarter	Bio9	°C
		Mean temperature of warmest quarter	Bio10	°C
		Mean temperature of coldest quarter	Bio11	°C
		Annual precipitation	Bio12	mm
		Precipitation of wettest month	Bio13	mm
		Precipitation of driest month	Bio14	mm
		Precipitation seasonality (coefficient of variation)	Bio15	Dimensionless
		Precipitation of wettest quarter	Bio16	mm
		Precipitation of driest quarter	Bio17	mm
		Precipitation of warmest quarter	Bio18	mm
		Precipitation of coldest quarter	Bio19	mm
Topographic	**USGS GTOPO30**	Elevation	elevation	m
		Aspect	aspect	Degree
		Slope	slope	Degree
	GEOFABRIK	Distance to water	dist_water	km
Vegetation-related	**MODIS 13Q1**	Mean Normalized Difference Vegetation Index	ndvi_mean	Dimensionless
	ICIMOD Land cover	Forest cover	forest	Dimensionless
Anthropogenic	**SEDAC**	Population density	pop_density	People km^{-2}
	GEOFABRIK	Distance to path	dist_path	km
	Survey Department Nepal	Distance to settlement	dist_settle	km
	Livestock Geo-Wiki	Livestock density	livestock_den	Livestock km^{-2}

Shapefiles of water resources, especially streams, were obtained from OpenStreetMap (https://www.openstreetmap.org/#map=5/51.509/-0.110). That was then subjected to analysis to compute the distance raster file using ArcGIS software.

Anthropogenic variables

A number of anthropogenic variables such as population density, road networks, and livestock density were identified as governing factors for forest fire (Singh and Zhu 2021). We acquired anthropogenic variables from the Socioeconomic Data and Application Center (SEDAC; CIESIN 2016); the data has 1-km spatial resolution. Furthermore, livestock density having the same resolution was obtained from Livestock Geo-Wiki (https://www.geo-wiki.org/; Robinson et al.

2014). Road and path networks were obtained from OpenStreetMap. The settlement points throughout Nepal were obtained from the Department of Survey, Nepal (https://www.dos.gov.np/). These datasets were subject to analysis to develop distance raster files of roads, paths, and settlements using ArcGIS.

Field-based dataset

In addition to remote-sensing-based data and secondary datasets from different sources, a key informant interview (KII) about historical fire incidents, their timing, aims of setting up fires, and impact at the local level was held with the representatives of local people and local officers from the Department of Forest, Government of Nepal, users communities' groups. Such KII were held in
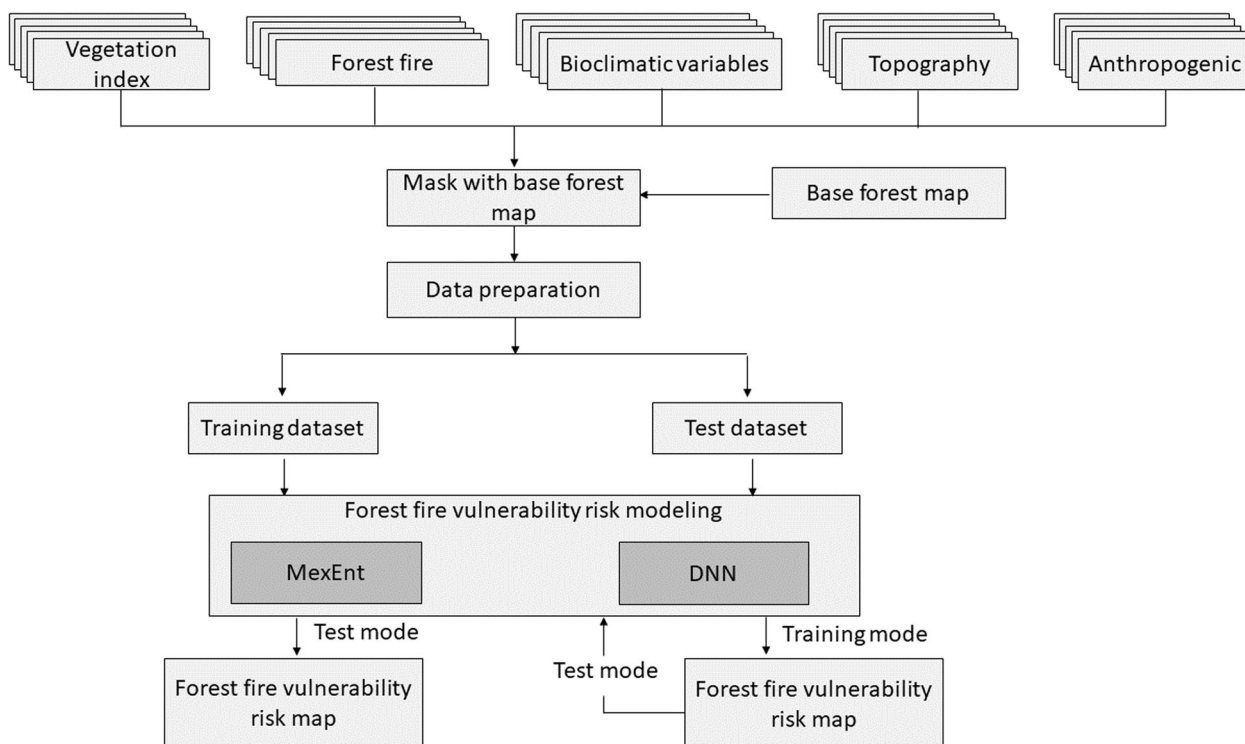
Fig. 3 Flow diagram for processing data used to model forest fire-vulnerability risk of Nepal

Kaski, Kailali, Baglung, Lamjung, Makawanpur, and Ilam in December 2020 and January 2021.

Data preparation

All non-forested areas were masked out of the land use and land cover map of Nepal, 2000 (ICIMOD 2018), so that we could work solely with the forested area time-series datasets for the country. All relevant remotely sensed data were downloaded for the study area, and we applied three different filters for the study area, data quality, and cloud coverage. A series of pre-processing steps were taken to get the stacked products clipped to the four physiographic regions of Nepal. This included the acquisition of forested area, acquisition of the fire-affected forested area, development of the fire-affected forest map, acquisition of the NDVI map, acquisition of the bioclimatic variable map, acquisition of the anthropogenic activity map, resampling all layers to match the resolution of the forest-fire map, and if necessary, co-registration and layer stacking that is ready for fitting the model. We used burned-area data from March through May of all years from 2000 through 2016. The overall methodological flow is provided in Fig. 3.

Statistical analysis

The burned-area data, the total surface area burned according to year and month in each physiographic region, were analyzed with descriptive statistics using R programming. The data were analyzed to reveal the trend and patterns in forest fires across physiographic zones. To explore the seasonal and temporal patterns, we performed a trend analysis of the forest-fire area based on yearly and monthly (average of all years, monthly) forest-fire area. Peak fire-affected months per physiographic zones were also computed.

We used the Mann-Kendall (MK) trend test method (Mishra et al. 2014) for the trend analysis of the fire-affected areas for the designated 16 years. In the hypothesis testing for trends, the null hypothesis is that there is no trend in the population from which the data set is drawn. The alternative hypothesis is that there is a trend in the population. The MK method is a non-parametric rank-based procedure, sensitive to the influence of extremes, and suitable for application with skewed variables. More particularly, this technique can be adopted in cases with no normally distributed time-series data, (i.e., data containing outliers and non-linear trends) (Karpouzos et al. 2010; Poudel and Shaw 2016). The statistical significance of the trend was determined based on the corresponding *P*-value.

Fire-vulnerability modeling

Fire-vulnerability modeling was performed using two approaches: MaxEnt, one of the most commonly used fire distribution modeling tools, and DNN, an emerging

Mishra *et al. Fire Ecology*   (2023) 19:3

Page 8 of 15

machine-learning approach that is reported to outperform many traditional machine-learning approaches in many thematic applications (Mishra et al. 2022). The following subsections describe the selection of input variables, data division for training and testing, and model fitting processes.

Selection of input variables

All of the 29 variables considered may not have been equally important for forest fire incidence and growth, and many of them may be interdependent on each other. Therefore, minimization of such redundant information is important, and one of the most common methods to do so is through the variance inflation factor (VIF), as shown in Eq. 1:

$$VIF_i = \frac{1}{1 - R_i^2},\tag{1}$$

where R_i^2 is the squared multiple correlations of the ith independent variable regressed on the other independent variables. VIF is computed iteratively and it removes the variable with the highest VIF value one at a time until all the variables have a VIF below the specific threshold value (<10, the most widely accepted value) (Kuo and Chang 2010; Campo-Bescós et al. 2013). We applied VIF to remove correlated metrics.

Furthermore, we used the 10-fold cross-validation approach while fitting the model, in which datasets from 2000 to 2016 were randomly split into 70% and 30%. Once fitted, the model's performance was evaluated and compared with the fire incident points from 2017 to 2019.

Maximum entropy

The MaxEnt model was implemented for forest fire-vulnerability risk modeling. We used 16 variables that incorporated bioclimatic, anthropogenic, topographic, and vegetation-related variables, and fire presence points to model forest fire-vulnerability risk area throughout the country (Table 2). For the best result, an ensemble of 10 results was considered as the outcome, as Barbet-Massin et al. (2012) recommended considering the aggregated results from 10 simulations for stable results.

Model evaluation was performed by two methods: threshold independent and threshold dependent. The area under the receiver-operator curve (AUC) is an independent method (Phillips et al. 2006). An AUC of <0.7 indicates poor model performance, 0.7 to 0.9 indicates moderate usefulness, and >0.9 denotes excellent model performance (Pearce and Ferrier 2000). Besides the AUC, threshold-dependent accuracy assessments (True Skill Statistic) were also performed to evaluate model performance (Allouche et al. 2006; Merow et al. 2013).

Table 2 Environmental variables selected for modeling forest fire-vulnerability risk of Nepal. Only those variables with a variance inflation factor of less than 10 were selected for modeling purposes. See Table 1 for corresponding variable units

Variable	VIF
Precipitation seasonality	9.40
Precipitation of the driest month	8.57
Annual precipitation	7.04
Precipitation of the driest quarter	5.56
Mean temperature of driest quarter	4.70
Livestock density	4.50
Annual temperature range	3.68
Normalized Difference Vegetation Index mean	2.82
Distance to path	2.43
Forest cover	2.33
Distance to settlement	2.27
Population density	2.25
Slope	2.23
Isothermality	1.99
Distance to water	1.35
Aspect	1.24

Deep neural network

A deep neural network (DNN), also called a stacked neural network, is a powerful set of techniques for learning in neural networks having more than one layer. During the learning process, it finds an appropriate function or manner of transferring from input to output. In predictive estimation, DNN can provide a multi-variate non-linear and non-parametric regression model for automatic estimation from the set of input parameters.

The layers are made up of nodes in which the actual computation happens. A node combines the input with a set of weights. These input-weight products ($w_i x_i$) are summed and passed through a node's activation function to predict the output. The weighted combination of input signals is aggregated and transmitted into an output signal, γ, as seen in Eq. (2):

$$\gamma = \sum_{i=1}^{n} w_i x_i + c,\tag{2}$$

where x_i is the input parameter, w_i is the corresponding weight, and c is the bias.

Activation is a mapping of input to the output through a non-linear transfer at each node in the network. The combination of weight and bias serves as input data from the previous layer to determine whether the signal surpasses a given threshold and is deemed significant. Those weights and biases are gradually updated only if the error is decreased. In this model, a widely accepted activation function, *tanh*, is used and shown in Eq. (3). The output values (*g*) can range from −1 to 1 in this activation function.

Mishra *et al. Fire Ecology*   (2023) 19:3

Page 9 of 15

Table 3 Optimum configuration parameter for the DNN model

Parameters	Values
Number of nodes in the input layer	Number of input features
Number of epochs	106
Distribution	Gaussian
Hidden layer	150,150,150
Activation function	adam
Input dropout ratio	0.1
L1	1e−5
L2	0
Rho	0.9

$$g_{\mathrm{tanh}} = \frac{e^x - e^{-x}}{e^x - e^{-x}}. \tag{3}$$

The model uses the Adam method for optimization. The Adam method computes individual adaptive learning rates for different parameters from estimates of the first and second moments of the gradients (Kingma and Ba 2015). The hyper-parameterization of the model was done with grid search; the hyper-parameters are shown in Table 3.

The continuous probability value map that ranges from 0 to 1 obtained from both MaxEnt and DNN was classified into four levels of risk: 0 to 0.25 = very low risk, 0.25 to 0.5 = low risk, 0.5 to 0.75 = high risk, and 0.75 to 1.0 = very high risk (Chen et al. 2015).

Accuracy assessment

The forested area across the country is classified into four categories of forest fire-vulnerability risk: very high, high, low, and very low. The forest fire events obtained from the Ministry of Forest and Environment, Department of Forest and Soil Conservation from 2017 to 2019 (DoF 2022), were used to access the accuracy of the outcome from both models. Fire events that fall in the high and very high vulnerability risk classes are considered to be truly detected fires; fire events that fall in the low and very low vulnerability risk classes are considered to be incorrectly detected. Using these two categories, true positive and true negative, we computed the probability of detection.

Results

Modern fire regime across Nepal

It has been observed that the majority of the burned area in Nepal is in the Chure zone, and the most concentration of burned area is in the western part of the country (Fig. 4a). Hills have relatively low fire occurrence, and the forest burn concentration decreased from west to east. About 78% of fire-affected areas burned more than once (i.e., same pixel) during the last 20 years, with the highest repeating frequency of two and then monotonically decreasing. In some places, the repetition was observed even in the same year (around 2% of the burned area), which might not be a forest fire incident in reality. These areas were excluded from the analysis.

On average, about 39,900 ha of forest, with about 25% of standard deviation, is burned every year. Years 2016, 2012, and 2001 were the biggest forest fire years, while the least fire incidence was observed in the years 2002 and 2014 (Fig. 4a). The statistics show that more than 78% of forest fires occurred from March to May (Fig. 4b), which drops to almost zero as soon as the rainy season starts in June, and no or very few fires are detected from then through September.

April incidents accounted for more than 43% of the fire-affected area. Referring to the historical dataset in
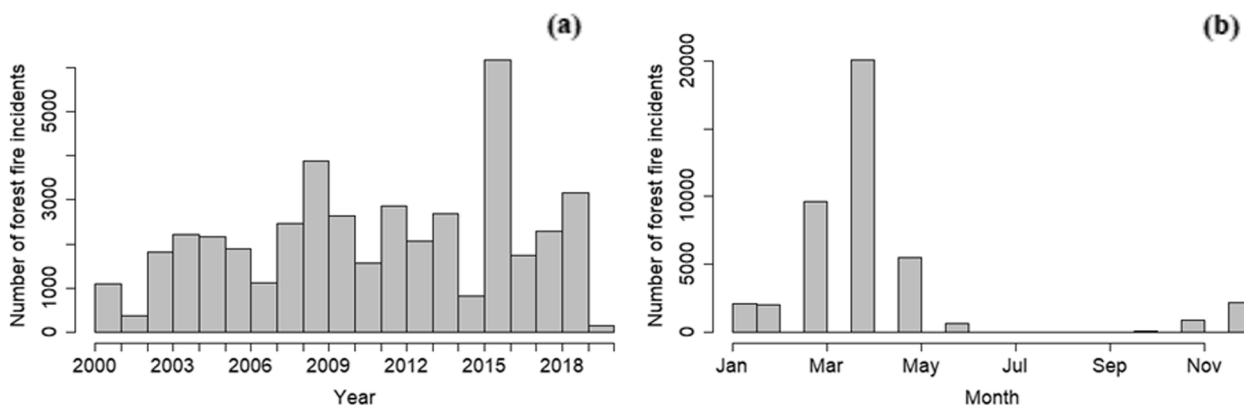

Fig. 4 Graphs of **a** yearly and **b** monthly forest fire incidents across Nepal from 2000 to 2019, generated from the MODIS data

Mishra *et al. Fire Ecology*   (2023) 19:3

Page 10 of 15

Table 4 Trend of change (slope) in annual burned area in Nepal during the months of March, April, and May, for four physiographical regions (High Mountain, Hill, Chure, and Terai), obtained from MODIS forest fire product. *P*-values are also given

Month	High Mountain		Hill		Chure		Terai	
	Slope	*P*-value	Slope	*P*-value	Slope	*P*-value	Slope	*P*-value
Mar	−8.717	0.343	1.146	0.417	1.188	0.893	0.458	0.160
Apr	0.917	0.528	1.879	0.588	**33.976**	**0.034**	0.641	0.685
May	0.550	0.222	2.000	0.321	**7.488**	**0.037**	4.125	0.174

Nepal, the majority of forest fire incidents and affected areas were recorded between March and May, 3 months of the year (Khanal 2015; Matin et al. 2017). Hence, it is worthwhile to focus the analysis on these 3 months.

We observed a general trend towards increasing forest fire in all 3 months in all four physiographical regions by as much as 33 ha per year over the 20 years of study data (see details in Table 4). The trend of increasing forest fire was highest in Chure and lowest in High Mountain. The trend of increasing forest fire area was decreasing in March. A significant trend of burned area (confidence interval = 95%) was observed only in Chure during April and May. For other regions, a statistically significant trend was not identified according to the MK test. Relatively greater burned area was found at lower elevations. More than 50% of the recorded fire area was at less than 1000-m elevation, which is mostly in the Terai and part of the Chure region. About 21% and 24% of the recorded forest fire area was between 1000 and 2000 m and 2000 and 3000 m in elevation, respectively, while the 3000- to 4000-m elevation range accounts for less than 5% of the recorded forest fire area. Hardly any forest fire area was recorded above 4000-m elevation.

Fire-vulnerability modeling
Figure 5 illustrates the forest fire-vulnerability risk obtained from DNN and MaxEnt across Nepal. The probability of detection using DNN was 0.71 while it was 0.64 using MaxEnt when accessing the results of forest fire events from 2017 to 2019 (DoF 2022). The summary of the accuracy assessment is presented in Table 5. The forest fire-vulnerability risk from both the DNN and MaxEnt models was comparable in terms of their distribution patterns (Fig. 5a, b) while using the same input dataset. The DNN model showed a much greater very-high-risk area than did the MaxEnt model (2.64% versus 0.27%). The high-risk area was comparable (i.e., 1.55% from DNN and 1.2% from the MaxEnt model). The MaxEnt model showed about 90% of the area under very low risk, while it was 83.78% from DNN. Thus, the MaxEnt model identified less area of high fire vulnerability than did the DNN model.

Twenty-nine remote-sensing metrics were evaluated for their dependency on forest-fire incidence. Out of 29, 17 variables had a VIF value of less than 10, and these were selected for the model development (Table 2). Among the selected 17 variables, bioclimatic variables were identified as more important and other variables (topographic, vegetation-related, and anthropogenic) as less important for fire-vulnerability modeling. Precipitation seasonality was the most important variable to modeling forest fire-vulnerability risk for MaxEnt. This variable has a permutation importance of 23.2 and 16.2% contribution. After precipitation seasonality, the mean temperature of the driest quarter, slope, and climate (isothermality) were important variables to modeling forest fire-vulnerability risk. These variables have permutation importance of 17.5, 8.6, and 8, respectively, in MaxEnt (Table 6). A comparable ranking was obtained with DNN modeling where precipitation seasonality, annual precipitation, mean temperature of driest quarter, and climate were the most important variables. The forest fire-vulnerability risk is low at lower land surface temperatures and high in areas having a high maximum and mean land surface temperature. Unlike the response to land surface temperature, forest fire-vulnerability risk is higher at a medium level of maximum and mean precipitation. Forest fire-vulnerability risk is low in areas with very low and very high precipitation. Low-precipitation areas are likely to have sparse vegetation cover, so the vulnerability of forest to risk of fire is also low.

Discussion
Based on both models, Chure and Terai in the western part of the country are more prone to potential fire in the future. The region was historically also vulnerable. These regions receive low rainfall compared with the eastern and central parts of the country. The western Terai plain, followed by the Chure area, has a higher probability of forest fire events than the Middle and High Mountains, which have the lowest probability of forest fire. Although bioclimatic factors were most prominent for the forest fire, topography also had some effects. The southern face of mountains is also more susceptible to forest fire than
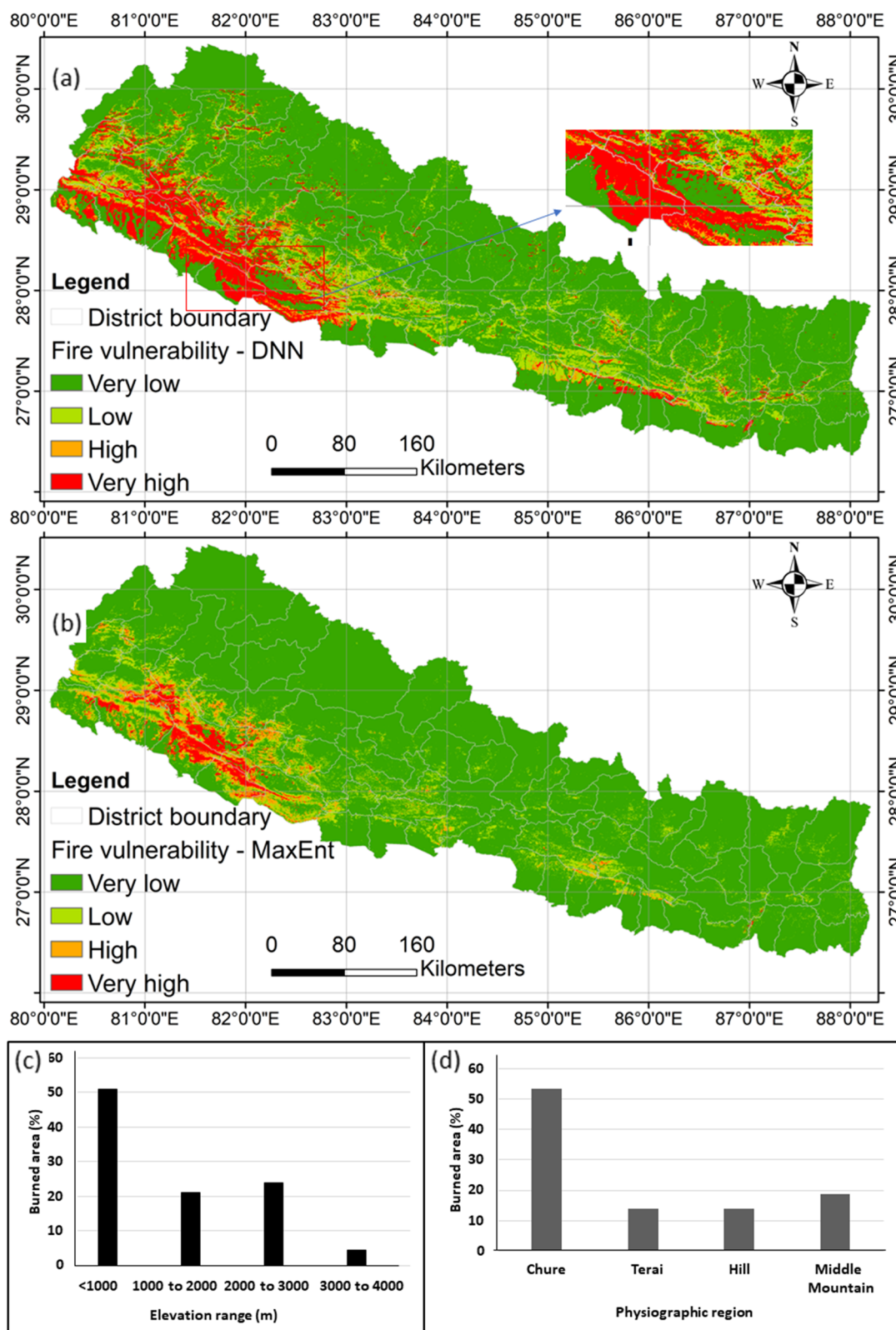
Fig. 5 Maps created by modeling forest fire-vulnerability risk across Nepal using historical forest fire incidents based on MODIS data, using the **a** deep neural network (DNN) approach, and the **b** Maximum Entropy (MaxEnt) approach. This same data was used to develop the graph of spatial distribution of **c** burned area across different elevation zones and **d** burned area across four physiographic zones of Nepal

Mishra *et al. Fire Ecology*   (2023) 19:3

Page 12 of 15

Table 5 Summary of accuracy assessment of vulnerability-risk models MaxEnt and DNN, based on forest fire events in 2017, 2018, and 2019. FALSE represents the number of incorrectly detected fire events. TRUE represents the number of truly detected forest fire events. The probability of detection was computed using the values in FALSE and TRUE

Method	Fire year	Forest fire-vulnerability risk class (*n*)				FALSE (*n*)	TRUE (*n*)	Probability of detection
		Very low	Low	High	Very high			
MaxEnt	2019	295	155	432	354	450	786	0.64
	2018	251	156	432	357	407	789	0.66
	2017	325	172	515	329	497	844	0.63
	Overall	**871**	**483**	**1379**	**1040**	**1354**	**2419**	**0.64**
DNN	2019	206	138	538	354	344	892	0.72
	2018	171	134	525	366	305	891	0.74
	2017	252	175	551	363	427	914	0.68
	Overall	**629**	**447**	**1614**	**1083**	**1076**	**2697**	**0.71**

Table 6 Percent contribution and relative importance of the variables used in DNN and MaxEnt modeling of forest fire-vulnerability risk of Nepal. See Table 1 for corresponding variable units

Variables	MaxEnt		DNN	
	Percent contribution	**Permutation importance**	**Relative importance**	**Percent contribution**
Precipitation seasonality	16.2	23.2	0.98	12.6
Mean temperature of driest quarter	1.5	17.5	0.14	7.7
Slope	5.9	8.6	0.2	2.9
Isothermality	3.3	8	0.11	10.6
Precipitation of the driest quarter	6.5	7.9	0.21	2.9
Annual precipitation	18.9	6.1	1	14.2
Population density	2.3	5.5	0.1	4.7
Temperature annual range	1.7	5.3	0.07	2.9
Distance to water	6.8	4.5	0.22	2.8
Precipitation of the driest month	2.7	2.8	0.13	6.9
Distance to path	8.6	1.8	0.25	7.1
Forest cover	11.6	1.7	0.31	9.4
Aspect	4.2	1.6	0.16	3.5
Livestock density	5	1.5	0.19	4.8
Distance to settlement	0.4	1.3	0.01	2.4
Normalized Difference Vegetation Index mean	4.3	1	0.14	5.5

any other face; south-facing areas had a higher fire frequency during the study period. As the south-face area is exposed to more sunlight, it consequently becomes dry. Forest fire incidence and burn area could be higher in such mountain areas. The higher concentration of forest fire incidents on the southern face of the Chure region is evidence of this increase.

March, April, and May are the most forest fire-prone months, which compose the driest and hottest season in the year, falling immediately after a prolonged cold and dry winter, when foliage is most susceptible to burn.

In addition, strong wind exacerbates fire events, adding more complexity to controlling fire. However, a significant portion of burned area at high elevations was recorded in November, December, and January.

In order to develop better forest management plans to protect the forest from fire damage, an up-to-date and accurate vulnerability assessment is needed to optimize the fuel management (Jain et al. 2020). Such an assessment would indicate the area most vulnerable to forest fire, so that fire management teams could prioritize fuel treatments and mitigation actions for better fuel

Mishra *et al. Fire Ecology*   (2023) 19:3

Page 13 of 15

management in the forest. Additionally, in the event of forest fire, the authority concerned could better manage the resources necessary to control the fire.

Similar to many other studies, the deep learning-based model (DNN) outperformed the MaxEnt model (Bjånes et al. 2021; Jain et al. 2020), although the pattern is very similar in both models in this study. The DNN model is better than MaxEnt in mountainous environments as it has a better fitting and classification ability than the traditional MaxEnt-based model due to its capacity in extracting complex features from very large input datasets through the full uses of the spatial context information (Bjånes et al. 2021; Jain et al. 2020; Mishra and Shahi 2021). The MaxEnt model works only with the presence data while fitting the model. Since fires do not occur in all places where fire-prone conditions exist, and it is difficult to define a true absence while training the model, there is the change of classifying fire-prone areas as less vulnerable that degrades the overall performance. In addition to that, the occurrence localities of training samples could have an impact in the outcome (Arnold et al. 2014). Additionally, the MaxEnt model often suffers from over-fitting that limits developing the generalized model with independent data due to its weak regularization mechanisms, which is more challenging in heterogeneous topography, such as Nepal. Conversely, DNN allows the implementation of several regularization techniques such as dropout, batch normalization, early stopping, and L1 and L2 regularization techniques which can better handle such issues and the network has the ability to capture complex relationships between input and output through a complex network.

Anthropogenic factors

Bioclimatic factors and topographic factors appeared more important than anthropogenic factors. This is due to the output dataset of the model, which is burned area, and the model accounts for the fire spreading conditions/burned area rather than ignition conditions. Additionally, fires in forested areas near small residential areas are often controlled by people and therefore may explain why anthropogenic factors are less important in the model. However, we discuss their potential influence in this study since they are known to influence ignition in other regions (Ganteaume et al. 2013).

During the KII in Bardiya, Ilam, Kaski, Lamjung, Makwanpur, and Baglung, local people and local officers of the department of forest agreed on the fact that people are motivated to set fires for two reasons, but there are not any record-keeping systems for such fire incidents in Nepal. Firstly, fires are set for the illegal poaching of wild animals; and secondly, fires are set to encourage the growth of better grasses for grazing. Large burned

areas in the Terai region occur mostly during the dry seasons, and the fires that cause them are likely to be intentionally set, although there is no evidence. The possible motivation for setting these fires could be for grazing, poaching, hunting, non-timber forest product collecting, and deforestation for land acquisition (Kunwar and Khaling 2006). Therefore, forests that are closer to more human activity (access to road, higher population density, higher livestock density, etc.) have a higher fire-vulnerability risk than that of remote forests. Similarly, remote, sparsely populated areas where governmental monitoring is not present could have an increased chance of forest fire caused by the intentional setting of fire by local people.

Conclusions

The forest fire-affected area in Nepal is highly seasonal, and the concentration of forest fire incidence is more in the western than in the eastern part of the country. Bioclimatic, vegetation index, topographic, and anthropogenic variables together define forest fire area and its vulnerability risk level. The southwestern part of the country was found to be more vulnerable to forest fire; it is more vulnerable in the Chure area of central Nepal and the hilly part of western Nepal as well. The forest fire-vulnerability risk maps will be helpful in understanding the risk pattern across the country. As the outcome of the model is in a raster format, we can generate variations of vulnerability risk maps to meet the needs of each administrative unit. Such maps are very useful to forest managers for allocating resources at the sub-national level based on relative risk and for developing strategies for forest-fire management. Similarly, these maps can help in the distribution of resources required to control forest fires. A further detailed study considering higher resolution forest fire and field data is recommended in the more vulnerable western region of the country where the frequency of fire is very high.

Authors' contributions
BM developed the analysis concept, interpreted statistics, and did the majority of manuscript writing; SP developed the analysis concept, compiled data, developed the MaxEnt model, created figures, and contributed to manuscript writing; SP performed the statistical analysis, analyzed data, and contributed to manuscript writing; BRG assisted in interpreting statistics and contributed to writing the manuscript. All authors read and approved the final manuscript.

Mishra *et al. Fire Ecology*   (2023) 19:3

Page 14 of 15

Availability of data and materials
All the data are from secondary sources and details of the data achieve are mentioned in the manuscript.

Declarations

Ethics approval and consent to participate
Not applicable.

Consent for publication
Not applicable.

Competing interests
The authors declare that they have no competing interests.

References

Allouche, O., A. Tsoar, and R. Kadmon. 2006. Assessing the accuracy of species distribution models: Prevalence, kappa and the true skill statistic (TSS). *Journal of Applied Ecology* 43: 1223–1232. https://doi.org/10.1111/j.1365-2664.2006.01214.x.

American Forest Foundation, 2015. Western water threatened by wildfire.

Andela, N., D.C. Morton, L. Giglio, Y. Chen, G.R. Van Der Werf, P.S. Kasibhatla, R.S. DeFries, G.J. Collatz, S. Hantson, S. Kloster, D. Bachelet, M. Forrest, G. Lasslop, F. Li, S. Mangeon, J.R. Melton, C. Yue, and J.T. Randerson. 2017. A human-driven decline in global burned area. *Science (80-.)* 356: 1356–1362. https://doi.org/10.1126/science.aal4108.

Aponte, C., W.J. De Groot, and B.M. Wotton. 2016. Forest fires and climate change: Causes, consequences and management options. *International Journal of Wildland Fire* 25: i–ii. https://doi.org/10.1071/WFv25n8_FO.

Arnold, J.D., S.C. Brewer, and P.E. Dennison. 2014. Modeling climate-fire connections within the great basin and upper Colorado River Basin, Western United States. *Fire Ecology* 10: 64–75. https://doi.org/10.4996/fireecology.1002064.

Bahadur, K.C., B.P. Heyojoo, Y.K. Karna, S.P. Sharma, and S. Panthi. 2017. Incidences of wildfire hazard and its effects on forest cover change in Chitwan National Park, Nepal. *Clarion: International Multidisciplinary Journal* 3: 51–60.

Barbet-Massin, M., F. Jiguet, C.H. Albert, and W. Thuiller. 2012. Modelling species distributions to map the road towards carnivore conservation in the tropics. *Methods in Ecology and Evolution*: 85–107. https://doi.org/10.1111/j.2041-210X.2011.00172.x.

Bhuju, U.R., P.R. Shakya, T.B. Basnet, and S. Shrestha. 2007. *Nepal biodiversity resource book protected areas, ramsar sites, and world heritage sites*. Kathmandu: Ministry of Environment, Science and Technology (MOEST), Government of Nepal (GoN) Singha Durbar.

Biswas, S., K.P. Vadrevu, Z.M. Lwin, K. Lasko, and C.O. Justice. 2015. Factors controlling vegetation fires in protected and non-protected areas of Myanmar. *PLoS One*: 1–18. https://doi.org/10.1371/journal.pone.0124346.

Bjånes, A., R. De La Fuente, and P. Mena. 2021. A deep learning ensemble model for wildfire susceptibility mapping. *Ecological Informatics* 65: 101397. https://doi.org/10.1016/j.ecoinf.2021.101397.

Boschetti, L., D. Roy, A.A. Hofmann, and M. Humber. 2008. MODIS collection 5 burned area product MCD45. *User's Guide* 3.0.1: 1–12. https://doi.org/10.1177/1937586718779219.

Bowman, D.M.J.S., and B.P. Murphy. 2010. Fire and biodiversity. In *Conservation biology for all*, 163–180.

Campo-Bescós, M.A., R. Muñoz-Carpena, J. Southworth, L. Zhu, P.R. Waylen, and E. Bunting. 2013. Combined spatial and temporal effects of environmental controls on long-term monthly NDVI in the Southern Africa Savanna. *Remote Sensing* 5: 6513–6538. https://doi.org/10.3390/rs5126513.

Chen, F., Y. Du, S. Niu, and J. Zhao. 2015. Modeling forest lightning fire occurrence in the Daxinganling Mountains of Northeastern China with MAXENT. *Forests* 6: 1422–1438. https://doi.org/10.3390/f6051422.

CIESIN. 2016. *Gridded population of the world, version 4.11 (GPWv4): Population count, revision 11 [WWW Document]. Revis. 11*. Palisades: NASA Socioecon. Data Appl. Cent. https://doi.org/10.7927/H4JW8BX5.

Cotton, James. 2014. The "haze" over Southeast Asia: Challenging the ASEAN Mode of Regional Engagement. *Pacific Affairs* 72: 331–351.

De Angelis, A., C. Ricotta, M. Conedera, and G.B. Pezzatti. 2015. *Modelling the meteorological forest fire niche in heterogeneous pyrologic conditions*, 1–17. https://doi.org/10.1371/journal.pone.0116875.

De Araújo, F.M., and L.G. Ferreira. 2015. Satellite-based automated burned area detection: A performance assessment of the MODIS MCD45A1 in the Brazilian savanna. *International Journal of Applied Earth Observation and Geoinformation* 36: 94–102. https://doi.org/10.1016/j.jag.2014.10.009.

Dobremez, J.F. 1976. *Le Népal: Écologie et biogéographie*. Paris: Éditions du Centre national de la recherche scientifique.

Doerr, S.H., and C. Santín. 2016. Global trends in wildfire and its impacts: Perceptions versus realities in a changing world. *Philosophical Transactions of the Royal Society B: Biological Sciences* 371. https://doi.org/10.1098/rstb.2015.0345.

DoF, 2022. Forest fire detection and monitoring system in Nepal [WWW Document]. http://nepal.spatialapps.net/NepalForestFire/EN

ESRI. 2017. *ArcGIS Desktop: Release 10.5*. Redlands: Environmental Systems Research.

FAO. 2020. *Global forest resources assessment 2020: Main report*. Rome: Reforming China's Healthcare System. https://doi.org/10.4060/ca9825en.

Fick, S.E., and R.J. Hijmans. 2017. WorldClim 2: New 1-km spatial resolution climate surfaces for global land areas. *International Journal of Climatology* 37: 4302–4315. https://doi.org/10.1002/joc.5086.

Fonseca, M., L. Alves, A.P. Aguiar, L. Anderson, and L. Aragão. 2017. Modelling future fire probability in the Brazilian Amazon under different land-use and climate change scenarios. In *Geophys. Res. Abstr. EGU Gen. Assem 19, 2017*, 10335.

Fornacca, D., G. Ren, and W. Xiao. 2017. Performance of three MODIS fire products (MCD45A1, MCD64A1, MCD14ML), and ESA Fire_CCI in a mountainous area of Northwest Yunnan, China, characterized by frequent small fires. *Remote Sensing* 9: 1–20. https://doi.org/10.3390/rs9111131.

FRA/DFRS. 2015. *State of Nepal's forests*, 50. Kathmandu: For. Resour. Assess.

Furlaud, J.M., L.D. Prior, G.J. Williamson, and D.M.J.S. Bowman. 2021. Bioclimatic drivers of fire severity across the Australian geographical range of giant Eucalyptus forests. *Journal of Ecology* 109: 2514–2536. https://doi.org/10.1111/1365-2745.13663.

Ganteaume, A., A. Camia, M. Jappiot, J. San-Miguel-Ayanz, M. Long-Fournel, and C. Lampin. 2013. A review of the main driving factors of forest fire ignition over Europe. *Environmental Management* 51: 651–662. https://doi.org/10.1007/s00267-012-9961-z.

Gentle, P. 1997. A study on forest fire at Bara district of the Nepal's Terai. *Banko Janakari, vol 7, 39 - 42*

Ghimire, B.R., M. Nagai, N.K. Tripathi, A. Witayangkurn, B. Mishara, and N. Sasaki. 2017. Mapping of Shorea robusta forest using time series MODIS data. *Forests* 8. https://doi.org/10.3390/f8100384.

GON. 2014. *Nepal fifth national report to convention on biological diversity*. https://doi.org/10.3109/03639048509056879.

Hernández Encinas, L., S. Hoya White, A. Martín del Rey, and G. Rodríguez Sánchez. 2007. Modelling forest fire spread using hexagonal cellular automata. *Applied Mathematical Modelling* 31: 1213–1227. https://doi.org/10.1016/j.apm.2006.04.001.

ICIMOD. 2018. *icimod_landcover_map_2000.pdf [WWW Document]*. ICIMOD http://geoapps.icimod.org/landcover/nepallandcover/.

Illera, P., A. Fernández, and J.A. Delgado. 1996. Temporal evolution of the NDVI as an indicator of forest fire danger. *International Journal of Remote Sensing* 17: 1093–1105. https://doi.org/10.1080/01431169608949072.

Jain, P., S.C.P. Coogan, S.G. Subramanian, M. Crowley, S. Taylor, and M.D. Flannigan. 2020. A review of machine learning applications in wildfire science and management. *Environmental Reviews* 28: 478–505. https://doi.org/10.1139/er-2020-0019.

Karpouzos, D.K., S. Kavalieratou, and C. Babajimopoulos. 2010. Trend analysis of precipitation data in Pieria Region (Greece). *European Water* 30: 31–40.

Kasischke, E.S., N.H.F. French, P. Harrell, N.L. Christensen, S.L. Ustin, and D. Barry. 1993. Monitoring of wildfires in boreal forests using large area AVHRR NDVI composite image data. *Remote Sensing of Environment* 45: 61–71. https://doi.org/10.1016/0034-4257(93)90082-9.

Khanal, S. 2015. Wildfire trends in Nepal based on MODIS burnt-area data. *Banko Janakari* 25: 76. https://doi.org/10.3126/banko.v25i1.13477.

Kim, S.J., C. Lim, G.S. Kim, J. Lee, T. Geiger, O. Rahmati, Y. Son, and W. Lee. 2019. Multi-temporal analysis of forest fire probability using socio-economic and environmental variables. *Remote Sensing* 11: 1–19. https://doi.org/10.3390/rs11010086.

Kingma, D.P., and J.L. Ba. 2015. ADAM: A method for stochastic optimization. In *ICLR*, 1–15.

Kunwar, R., and S. Khaling. 2006. Forest fire in the Terai, Nepal: Causes and community management interventions. *International Forest Fire News* 34: 46–54.

Kuo, Y.M., and F.J. Chang. 2010. Dynamic factor analysis for estimating ground water arsenic trends. *Journal of Environmental Quality* 39: 176–184. https://doi.org/10.2134/Jeq2009.0098.

Leuenberger, M., J. Parente, and M. Tonini. 2018. Environmental modelling & software wild fire susceptibility mapping: Deterministic vs. stochastic approaches. *Environmental Modelling & Software* 101: 194–203.

Lopes, M., and J.A.T. Machado. 2014. Dynamic analysis and pattern visualization of forest fires. *PLoS One* 9. https://doi.org/10.1371/journal.pone.0105465.

Luintel, N., W. Ma, Y. Ma, B. Wang, J. Xu, B. Dawadi, and B. Mishra. 2021. Tracking the dynamics of paddy rice cultivation practice through MODIS time series and PhenoRice algorithm. *Agricultural and Forest Meteorology* 307: 108538. https://doi.org/10.1016/j.agrformet.2021.108538.

Makhaya, Z., J. Odindi, and O. Mutanga. 2022. The influence of bioclimatic and topographic variables on grassland fire occurrence within an urbanized landscape. *Scientific African* 15: e01127. https://doi.org/10.1016/j.sciaf.2022.e01127.

Martín, Y., M. Zúñiga-antón, M.R. Mimbrero, and Y. Mart. 2019. Modelling temporal variation of fire-occurrence towards the dynamic prediction of human wildfire ignition danger in northeast Spain in northeast Spain. *Geomatics, Natural Hazards and Risk* 10: 385–411. https://doi.org/10.1080/19475705.2018.1526219.

Matin, M.A., V.S. Chitale, M.S.R. Murthy, K. Uddin, B. Bajracharya, and S. Pradhan. 2017. Understanding forest fire patterns and risk in Nepal using remote sensing, geographic information system and historical fire data. *International Journal of Wildland Fire* 26: 276–286.

Merow, C., M.J. Smith, and J.A. Silander. 2013. A practical guide to MaxEnt for modeling species' distributions: What it does, and why inputs and settings matter. *Ecography (Cop.)* 36: 1058–1069. https://doi.org/10.1111/j.1600-0587.2013.07872.x.

Miquelajauregui, Y., S.G. Cumming, and S. Gauthier. 2016. Modelling variable fire severity in boreal forests: effects of fire intensity and stand structure. *PLoS One* 11. https://doi.org/10.1371/journal.pone.0150073.

Mishra, B., M.S. Babel, and N.K. Tripathi. 2014. Analysis of climatic variability and snow cover in the Kaligandaki River Basin, Himalaya, Nepal. *Theoretical and Applied Climatology* 116: 681–694. https://doi.org/10.1007/s00704-013-0966-1.

Mishra, B., A. Dahal, and N. Luintel. 2022. Methods in the spatial deep learning: Current status and future direction. *Spatial Information Research* 30. https://doi.org/10.1007/s41324-021-00425-2.

Mishra, B., and T.B. Shahi. 2021. Deep learning-based framework for spatiotemporal data fusion: An instance of Landsat 8 and Sentinel 2 NDVI. *Journal of Applied Remote Sensing* 15: 1–13. https://doi.org/10.1117/1.jrs.15.034520.

Nelson, A., and K.M. Chomitz. 2011. Effectiveness of strict vs. multiple use protected areas in reducing tropical forest fires: A global analysis using matching methods. *PLoS One* 6. https://doi.org/10.1371/journal.pone.0022722.

Parajuli, A., A.P. Gautam, S.P. Sharma, K.B. Bhujel, G. Sharma, P.B. Thapa, B.S. Bist, and S. Poudel. 2020. Forest fire risk mapping using GIS and remote sensing in two major landscapes of Nepal. *Geomatics, Natural Hazards and Risk* 11: 2569–2586. https://doi.org/10.1080/19475705.2020.1853251.

Pearce, J., and S. Ferrier. 2000. Evaluating the predictive performance of habitat models developed using logistic regression. *Ecological Modelling* 133: 225–245. https://doi.org/10.1016/S0304-3800(00)00322-7.

Phillips, S.B., V.P. Aneja, D. Kang, and S.P. Arya. 2006. Modelling and analysis of the atmospheric nitrogen deposition in North Carolina. *International Journal of Global Environmental Issues* 6: 231–252. https://doi.org/10.1016/j.ecolmodel.2005.03.026.

Poudel, S., S. Funakawa, and H. Shinjo. 2017. Household perceptions about the impacts of climate change on food security in the mountainous region of Nepal. *Sustainability* 9: 641. https://doi.org/10.3390/su9040641.

Poudel, S., S. Funakawa, H. Shinjo, and B. Mishra. 2020. Understanding households' livelihood vulnerability to climate change in the Lamjung district of Nepal. *Environment, Development and Sustainability* 22. https://doi.org/10.1007/s10668-019-00566-3.

Poudel, S., and R. Shaw. 2016. The relationships between climate variability and crop yield in a mountainous environment: A case study in Lamjung District, Nepal. *Climate* 4: 13. https://doi.org/10.3390/cli4010013.

Renard, Q., R. Ṕlissier, B.R. Ramesh, and N. Kodandapani. 2012. Environmental susceptibility model for predicting forest fire occurrence in the Western Ghats of India. *International Journal of Wildland Fire* 21: 368–379. https://doi.org/10.1071/WF10109.

Robinne, F.N., 2021. Impacts of disasters on forests, in particular forest fires, UNFFS Background paper.

Robinson, T.P., G.R. William Wint, G. Conchedda, T.P. Van Boeckel, V. Ercoli, E. Palamara, G. Cinardi, L. D'Aietti, S.I. Hay, and M. Gilbert. 2014. Mapping the global distribution of livestock. *PLoS One* 9: e96084. https://doi.org/10.1371/journal.pone.0096084.

Singh, M., and X. Zhu. 2021. Analysis of how the spatial and temporal patterns of fire and their bioclimatic and anthropogenic drivers vary across the Amazon rainforest in El Niño and non-El Niño years. *PeerJ* 9. https://doi.org/10.7717/peerj.12029.

Vilar, L., I. Gómez, J. Martínez-vega, P. Echavarría, and D. Ria. 2016. Multitemporal modelling of socio-economic wildfire drivers in central Spain between the 1980s and the 2000s: Comparing generalized linear models to machine learning algorithms. *PLoS One* 11: 1–17. https://doi.org/10.1371/journal.pone.0161344.

Zhang, G., M. Wang, and K. Liu. 2019. Forest fire susceptibility modeling using a convolutional neural network for Yunnan province of China. *International Journal of Disaster Risk Science* 10: 386–403. https://doi.org/10.1007/s13753-019-00233-1.

Zhang, G., M. Wang, and K. Liu. 2021. Deep neural networks for global wildfire susceptibility modelling. *Ecological Indicators* 127: 107735. https://doi.org/10.1016/j.ecolind.2021.107735.

Publisher's Note